Preparation and characterization of composites based on poly(lactic acid)/poly(methyl methacrylate) matrix and sisal fiber bundles: the effect of annealing process

Ander Orue,[1] Jon Anakabe,[2] Ane Miren Zaldua-Huici,[2] Arantxa Eceiza,[1] Aitor Arbelaiz[1]

[1]'Materials + Technologies' Group (GMT), Chemical & Environmental Engineering Dept., Faculty of Engineering, Gipuzkoa, University of the Basque Country UPV/EHU, Pza. Europa 1, 20018 Donostia-San Sebastian, Spain

[2]Leartiker S. Coop., Xemein etorbidea 12, 48270 Markina-Xemein, Spain

Corresponding author: Aitor Arbelaiz, 'Materials + Technologies' Group (GMT), Chemical & Environmental Engineering Dept., Faculty of Engineering, Gipuzkoa, University of the Basque Country UPV/EHU, Pza. Europa 1, 20018 Donostia-San Sebastian, Spain

Email: aitor.arbelaiz@ehu.eus

Abstract

The interest on poly(lactic acid)/poly(methyl methacrylate) blends has increased during the last years due to their promising properties. The novelty of the current work focuses on the preparation and characterization of biocomposites based on poly(lactic acid)/poly(methyl methacrylate) matrix and NaOH treated sisal fibers. The effect of the addition of treated sisal fibers on the physico-mechanical properties of high polylactide

content composites was studied. For this purpose, poly(lactic acid)/poly(methyl methacrylate) blend (80/20 wt%) was prepared by melt-blending and reinforced with different fiber contents. Although composites showed interesting specific tensile properties, the estimated heat deflection temperature (HDT), i.e., the maximum temperature at which a polymer system can be used as a rigid material, barely increased 4 ºC respect to unreinforced system. After the annealing process, the heat deflection temperature of the unreinforced polymer blend increased around 25 ºC whereas the composites showed an increase of at least 38 ºC. Nonetheless, the specific tensile strength of composite decreased approximately 48 % because the adhesion between fiber and polymer matrix was damaged and cracks were formed during annealing process.

Keywords

Sisal fiber; Composite; Tensile properties; Thermomechanical properties; Annealing

1. Introduction

The huge consumption of plastics involves the generation of wastes that are difficult to manage from the environmental point of view. This fact has supported the need of continuous scientific research and development of more sustainable materials than that are currently used in the industry. The development of materials derived from renewable sources has generated much interest [1,2]. In this framework, lignocellulosic fibers obtained from different plants show interesting specific properties that make them interesting for using as reinforcement in polymeric matrices. The topic of composites based on cellulosic fibers has been widely studied [3,4,5,6,7,8,9] since they are easily processable, show lower carbon footprint than conventional synthetic materials, and

offer interesting specific properties. The specific properties of the natural fiber composites are, in some cases, superior to composites reinforced with glass fiber[10]. Therefore, natural fiber composites could replace composites reinforced with glass fiber in many applications where very high load bearing capabilities are not required [11].These composites could be an interesting option for automotive industry, since they represent significant weight savings in automotive pieces, respect to glass fibers, which lead to cost savings on fuel consumption and decrease in pollution 4. For example, Kumar and Das 4 reinforced poly(lactic acid) (PLA) with nettle fibers and they concluded that PLA/lignocellulosic fiber composite showed high potential for automotive dashboard panel application. Pappu et al.[12] concluded that high performance hybrid fiber reinforced composites can be manufactured using sisal and hemp fibers in combination with polylactic acid by extrusion and injection molding techniques. Pereira et al.[13] studied the mechanical performance of thermoplastic olefin composites reinforced with coir and sisal natural fibers concluding that the prepared composites were a valuable material for automotive applications.

PLA polymer, derived from renewable resources, is an interesting candidate for composite matrix. PLA is compostable and shows attractive physico-mechanical properties in terms of tensile strength and stiffness. Nevertheless, PLA shows poor impact strength and low heat distortion temperature 6. To overcome the drawbacks of PLA, many attempts have been reported in the literature[14-20]. Recently, poly(methyl methacrylate) (PMMA) has received great interest as a blend candidate for PLA due to its higher glass transition temperature and complementary mechanical properties [14,21,22]. The study of composites based on PLA/PMMA blend matrix and reinforced with short fibers is a quite new topic. Cousins et al. manufactured PLA/PMMA blend reinforced with chopped glass fiber using a twin-screw extrusion, and they concluded that the

addition of chopped glass fiber increased the mechanical properties of PLA/PMMA blend. Nevertheless, the novelty of current work is the preparation and characterization of biocomposites based on PLA/PMMA matrix with high polylactide content and reinforced with treated sisal fibers. Even though PMMA is a non-degradable petrochemical polymer, at least the 84 wt% of total amount of material are bio-based materials. The development of these kind of materials would be a good approach to continue researching novel biocomposites that are more sustainable and eco-friendlier materials than that are currently used. Thus, the main goal of the current work is to study the effect of treated sisal fiber addition and fiber content on physico-mechanical properties of composites based on PLA/PMMA matrix with high polylactide content. In addition, the properties of new biocomposites are compared with literature data of thermoplastic composites that are commonly used in different industrial applications such as automotive. Besides, the effect of annealing process on the mechanical and thermomechanical properties of prepared composites was studied.

2. Experimental part

2.1. Materials

PLA was purchased from NatureWorks LLC (Ingeo^{TM} 3051D, M_n = 106,000 g/mol; PDI: 1.7; ≈4.6 % D-lactate) and PMMA from Evonik ROM GmbH (PLEXIGLAS® zk5BR, M_n = 70,000 g/mol; PDI: 2.3). The molecular weights and molecular weight distribution of both materials were previously determined by gel permeation chromatography [14].

Sisal, *Agave sisalana*, fiber bundles cultivated in Africa were kindly supplied by Celulosa de Levante S.A. (Tortosa, Spain). The diameter values of untreated sisal fibers varied between 100 and 250 μm [19]. The chemical composition of raw sisal fibers was

earlier determined [23]. Fiber uniform size fraction was prepared according to TAPPI T257 cm-85 standard. Acid-insoluble lignin of fibers was determined using the TAPPI T222 om-02 standard. The holocellulose content was determined using the method proposed by Wise et al. [24]. Using the procedure proposed by Rowell et al. [25], α-cellulose was determined and by the difference between the values of holocellulose and α-cellulose the hemicellulose content of the fibers was calculated.The cellulose, hemicellulose and lignin content of the fibers was around 63 %, 12 % and 8 %, respectively. Sodium hydroxide pellets, supplied by Panreac, were used as fiber surface modifier and NaOH treatment of fibers was carried out based on an earlier work [26]. It was observed that NaOH treatment is an effective method to improve the adhesion and wettability between the sisal fibers and PLA matrix [19,26]. In brief, sisal fibers were treated with a 2 wt% NaOH solution for 12 h at room temperature followed by a more severe treatment with 7.5 wt% NaOH solution at 100 ºC for 90 min. Finally, sisal fibers were washed and dried for 12 h at 100 ºC. On the other hand, tetrahydrofuran (THF) supplied by Macron Fine Chemicals was used to dissolve the polymer matrix.

2.2. Compounding and processing of materials

Figure 1 shows the schemetic diagram of different steps involved in the manufacturing of composites. First, PLA and PMMA were dried for 4 h at 80 ºC in an oven before blending, PLA/PMMA 80/20 (wt%) composition was chosen as the thermoplastic matrix because this blending ratio showed the highest thermal stability, tensile strength and elastic modulus values among all studied compositions [14].

Manually premixed PLA and PMMA pellets were melt-blended in a HAAKE Rheomix 600 internal mixer (Thermo Scientific, Karlsruhe, Germany) with two Banbury rotors at 215 ºC with a rotor speed of 50 rpm for 4 min. Once PLA/PMMA (80/20 wt%) blend

was obtained, NaOH treated sisal fibers, previously dried for 12 h at 90 ºC, were added in the internal mixer at 215 ºC and all systems were mixed during 5 min at 50 rpm after the all the fiber content was introduced in the melt mixer. Composites with different fiber content, 20, 30 and 40 wt%, were prepared. Afterwards, blends were cooled-down until room temperature and pelletized by the cutting mill SM200 (RETSCH, Hann, Germany). All pelletized samples were kept in an oven at 90 ºC for 12 h prior to obtain tensile test specimens (ASTM-D638-10, type V) by means of a HAAKE Minijet II injection machine (Thermo Scientific, Karlsruhe, Germany). The selected injection and mold temperature values were 215 ºC and 75 ºC, respectively, while the molding pressure was set at 850 bar at 8 s.

2.3. Characterization

2.3.1. Density measurements

Density measurements of unreinforced polymer blend and its composites were carried out according to ASTM-D3800-16 standard in an AJ50L analytical balance (Mettler Toledo, Columbus, Ohio, USA). Sample was weighed in air and then in canola oil, and the weight difference between two media was the buoyancy force [19,27]. Sample density, ρ_s, was determined using Eq. (1):

$$\rho_s = \left(\frac{M_1}{M_1 - M_2} \right) \left(\rho_{canola} - \rho_{air} \right) + \rho_{air} \qquad (1)$$

where M_1 is the weight of sample in air, M_2 is the weight of sample in canola oil, ρ_{canola} is the density of canola oil and ρ_{air} is the density of air. The density value of canola oil and the air was 0.9155 g/cm^3 and 0.0012 g/cm^3, respectively. Density value of samples was averaged from at least three measurement data.

2.3.2. Tensile test

Tensile tests were performed according to ASTM D638 standard using Insight 10 testing system (MTS Company, Eden Prairie, Minnesota, USA) equipped with a load cell of 10 kN and pneumatic grips. Tests were performed at 1 mm/min deformation rate and the deformation of tensile specimen was determined using a video extensometer. Tensile properties were averaged from at least five test specimen data. Tensile strength and modulus values were divided by the measured density value for each system in order to calculate mass-specific values.

2.3.3. Unnotched impact test

Unnotched Charpy impact tests were carried out by IMPats-15 impact pendulum (ATS Faar, Novegro-Tregarezzo, Milan, Italy) with a 2 J hammer and a support span of 40 mm. Even though sample geometry used for impact test did not follow any standards, for comparison purposes, injection molded V type specimens were cut to a length of 63.5 mm and a constant section of 3.18 x 3.29 mm^2. At least five specimens were tested for each system and the mean values are reported.

2.3.4. Scanning electron microscopy

SEM micrographs were performed by JSM-6400 equipment (JEOL, Tokyo, Japan) with a wolfram filament operating at an accelerated voltage of 20 kV. Impact fractured surface of unreinforced polymer blend and composites was coated with gold using Q150 TES metallizer (Quorum Technologies Ltd, Laughton, England).

2.3.5. Fiber length and diameter measurements

To investigate how the compounding process affects fiber dimensions, the matrix of injection molded specimen was dissolved in THF under reflux. At least 400 fibers

length and diameter values were measured using an Eclipse E600W optical microscopy (Nikon, Tokyo, Japan).

2.3.6. Differential scanning calorimetry

Thermal properties were investigated by differential scanning calorimetry (DSC) using DSC 822e equipment (Mettler Toledo, Columbus, Ohio, USA). Samples with a weight between 5 and 10 mg were subjected to two heating-cooling cycles from 20 ºC to 170 ºC under a nitrogen atmosphere. In order to remove the thermal history, the first heating and cooling scans were carried out at 10 ºC/min, whereas the second heating scan was taken out at 3 ºC/min. The degree of crystallinity (χ_c) was determined according to Eq. (2):

$$\chi_c = \left(\frac{\Delta H_m - \Delta H_{cc}}{\Delta H_{100\%} \times w_{PLA}} \right) \times 100 \quad (2)$$

where ΔH_m is the enthalpy of melting process, ΔH_{cc} is the enthalpy of cold-crystallization process, $\Delta H_{100\,\%}$ is the melt enthalpy for theoretical 100 % crystalline PLA and w_{PLA} is the weight fraction of PLA. In the current work, a value of 93 J/g was taken as the melt enthalpy of 100 % crystalline PLA [28]. The area under the exothermic peak and endothermic peak are settled as ΔH_{cc} and ΔH_m, respectively. DSC analysis were performed in duplicate.

2.3.7. Dynamic-mechanical analysis

Dynamic-mechanical analysis (DMA) tests of unreinforced polymer blend and its composites were performed using an ARES rheometer manufactured by Rheometric Scientific (currently TA Instruments, New Castle, Delaware, USA). The temperature

was varied from 30 to 150 ºC while the rheometer was operating in torsion mode at a frequency of 1.6 Hz and a strain of 0.005 %. DMA tests were performed in duplicate.

2.4. Statistical analysis

The statistical analysis of the data was performed using one-way analysis of variance (ANOVA) in the OriginPro (Version 9.0) software program. Differences between pairs of means were determined by the Tukey´s test with the level of significance set at $P < 0.05$.

3. Results and discussion

3.1. Properties of non-annealed PLA/PMMA-based systems

3.1.1. Density data

The density value of systems was determined to calculate the specific tensile properties. Unreinforced polymer blend showed a density value of 1.232 g/cm^3 whereas the density value of composites increased together with the fiber content. Thus, the density value obtained for composites based on 20, 30 and 40 wt% fiber was 1.274 g/cm^3, 1.300 g/cm^3 and 1.314 g/cm^3, respectively. All density values were significantly different ($P < 0.05$) through the Tukey's multiple range test.

3.1.2. Specific tensile properties

The specific tensile properties of unreinforced polymer blend and its composites based on treated sisal fibers are shown in Figure 2 a-c. It was observed that strength value increased with increasing the fiber content, suggesting that the stress is transferred from the matrix to the fibers. On the other hand, the incorporation of sisal fibers led to a material with higher modulus than unreinforced matrix one. This fact is attributed to the

stiffness imposed in the composite by the sisal fiber. However, the presence of fibers restricted the strain capacity of matrix, reducing the deformation at break value. Nanthakumar et al. [29] prepared poly(lactic acid) /sugarcane leaves fiber biofilms via a solvent-casting method. Similarly, they observed that the tensile strength and Young's modulus of biofilms increased with the increasing of fiber content whereas the elongation at break decreased.

It was observed for composites containing 40 wt% of fibers that specific tensile strength and modulus values increased around 22 % and 88 %, respectively, whereas the elongation at break value decreased approximately 74 % respect to unreinforced polymer blend. A similar trend was observed for composites based on different thermoplastic polymers and natural fibers [19,30,31].

3.1.3. Unnotched impact test

Figure 3 shows the impact strength value of the unreinforced polymer blend and its composites. The unreinforced blend showed an impact strength value around of 10.5 kJ/m^2 and it decreased down to around 7.3 kJ/m^2 after the addition of sisal fibers regardless the fiber content. The reduction of impact strength values was observed for a wide range of polymeric matrices reinforced with organic or inorganic fibers [4,17,30,32,33]. Probably, the incorporation of fiber into matrix hinder the mobility of PLA/PMMA matrix and consecuently reduces the capability of composites to absorb energy during crack propagation. Furthermore, stress concentrations may occur at regions around fiber ends which could reduce the impact strength [34]. Contrarily, Cousins et al. [22] observed that the impact strength value of notched PLA/PMMA blend (75/25 wt%) specimens increased from 1.7 kJ/m^2 to 4.4 kJ/m^2 after the addition of 40 wt% chopped glass fibers. It is suggested in the literature that the fiber dimensions, fiber composition, manufacturing and preparation of the fibers as well as damage throughout the

compounding and molding process are important factors that could modify the impact properties of composites [3,4,35]. For example, Perez-Fonseca et al. [36] observed that the impact strength of PLA (30 J/m) increased with the addition of agave or coir fibers, reaching values of 35 and 40 J/m for fiber contents of 20 and 30 %, respectively. However, when pine fibers were incorporated to PLA, they did not observe impact strength improvement. According to Perez-Fonseca et al. [36] agave and coir fibers were much longer than pine fibers and the length of the reinforcement would be the reason for obtaining such different results.

3.1.4. Scanning electron microscopy

SEM micrographs of impact fractured surface of the unreinforced polymer blend and the composite containing 30 wt% of sisal fiber are shown in Figures 4-5. The fracture surface of unreinforced PLA/PMMA blend (Figure 4a) is characterised by the presence of different zones: (a) a flat mirror zone; (b) a transition zone, where the surface roughness increases and (c) a final propagation zone. The presence of the mirror zone in the unreinforced PLA/PMMA blend suggests a brittle fracture of the unreinforced system. In Figure 4b a dispersed PMMA-rich phase (< 400 nm in diameter) was observed evenly distributed in the continuous PLA-rich phase. The impact fractured surface depicted in these micrographs have similar morphology to those observed by Anakabe et al. [14] and Imre et al. [37]. Nevertheless, in contrast to the morphology observed in the current work, other authors [22,38,39] observed a co-continuous morphology, probably because they used different preparation process conditions and/or polymers with different molecular weight compared to those used in the current study. SEM micrographs of the composite blend, Figure 5a, showed a rough and serrated surface. Moreover, it seemed that the NaOH treated sisal fibers were covered with polymer matrix (see arrows in Figure 5b) suggesting that the wettability and adhesion

between the treated fibers and the polymer matrix is good. It was previously observed [26] that NaOH treatment, not only improve the wettability of sisal fibers with PLA, but also improved the PLA/fiber interfacial shear strength. On the other hand, the addition of fibers did not alter the coexistence of two separated polymeric phases (Figure 5c).

3.1.5. Fiber breakage analysis

The length and diameter values of fibers after processing were fitted to Log Normal frequency distribution. Table 1 reports the mean length and diameter values of sisal fibers obtained after processing. The length and diameter of the fibers decreased after the processing step, becoming thinner and smaller as the fiber content was increased in the composites. Compared to the values obtained for PLA/sisal fiber composites [19], the length and diameter values of sisal fibers in the composites based on PLA/PMMA matrix were smaller, at least 40 % and 75 %, respectively. A possible reason for obtaining lower values than in PLA/sisal fiber composites could be the higher viscosity of PLA/PMMA blend than PLA matrix system, which could lead to a more important fiber breakage level.

3.1.6. Differential scanning calorimetry

Cooling and second heating scans of DSC thermogram of unreinforced polymer blend and composites are shown in Figure 6. Regardless of the fiber content, no crystallization was observed during the cooling step and consequently samples were almost amorphous. In agreement with the observation done earlier [14], after melting the unreinforced polymer blend showed a single glass transition temperature at around 57.7 ºC, suggesting good miscibility between PLA and PMMA. On the other hand, no (or just a negligible) cold-crystallization process was observed during the subsequent heating scan, suggesting that the crystallization kinetics of the blend was slow due to the

presence of PMMA [14]. Cousins et al. [22] observed similar results for PLA/PMMA polymer blend (75/25 wt%).

After the addition of fiber, composites were almost amorphous and the T_g value remained close to that of the unreinforced system. Composite based on 30 wt% fiber content shows cold-crystallization during heating scan and consequently, these crystals showed a melting peak. On the other hand, composites with 20 % or 40 % fiber contents do not show neither cold-crystallization nor melting peak. Irrespective to fiber content, all composites were amorphous previous to the second heating scan.

3.1.7. Dynamic-mechanical analysis

Figure 7 a-c shows the variation of the storage modulus, loss modulus and tan δ values of unreinforced polymer blend and its composites. The presence of fiber in PLA matrix restricts the mobility of PLA chains and thus increases the stiffness of the composites which is in agreement with the findings by Khoo and Chow [40] for poly(lactic acid)/sugarcane bagasse fiber composites. After a constant region, a sharp storage modulus reduction was observed around 70 ºC related to the glass transition of amorphous regions [41,42,43].

Above the T_g, the increase of storage modulus value related to cold-crystallization was not very obvious in the unreinforced blend. In contrast, the reinforced systems showed an increase in their modulus values due to the cold-crystallization process promoted by fibers [18]. A higher storage modulus value in the whole studied temperature range was shown as the fiber content increased in the systems, whereas the differences in the loss modulus value were especially perceptible in the rubbery state (above T_g). Cousins et al. [22] observed a similar trend when they reinforced PLA/PMMA polymer blend with 40 wt% of chopped glass fibers. Nevertheless, the E´ values obtained by Cousins et al. [22] were higher than those results obtained for composites based on treated sisal fibers due

to the high modulus values of glass fiber. Regarding the tan δ values, Figure 7c, after the addition of treated sisal fibers the T_g value of the PLA-rich phase slightly decreased from 70 ºC to 68 ºC. The second T_g, corresponding to PMMA-rich phase, was not observed probably because it was hidden behind the cold-crystallization process of PLA. The tan δ peak height of neat PLA/PMMA blend decreased considerably after the addition of treated sisal fibers.

3.1.8. Comparison with literature data

Table 2 summarizes different property values of the composites prepared in the current study together with the properties of other reinforced systems reported in literature. Mineral filled polypropylene (PP) composites, which are usually used in the automotive industry, are included. Among other parameters, the mechanical properties of composites depend on the volumetric fraction of reinforcement. For comparative purpouses, all data are referred to reinforcement volume fraction. The prepared PLA/PMMA composites based on 20, 30 and 40 wt% treated sisal fibers correspond to 18, 27 and 36 % of reinforcement volume fraction, respectively.

Comparing similar reinforcement volume fractions, it can be observed that the specific strength values of composites prepared in the current work are similar or higher than those reported by other authors. Among the composites containing around 18 % of reinforcement volume fraction, the composite prepared in the current study shows at least a 50 % higher specific strength value than mineral filled PP systems [44,45]. Furthermore, the modulus value of PLA/PMMA composite is, in general, higher than for mineral filled PP systems. However, PLA/PMMA composite reinforced with treated sisal fibers showed lower elongation at break values than composites reinforced with mineral filler ones.

When PLA/PMMA matrix composites with around 25 vol% of reinforcement are compared, it was observed that composites with sisal fibers showed similar specific strength values to composites prepared with chopped glass fibers by Cousins eta al. [22]. However, the specific modulus of the composite with sisal fiber was the half of those composites reinforced with glass fibers. These results did not correspond with the differences of strength ratio and modulus ratio between glass fiber and NaOH treated sisal fibers. It was estimated that NaOH treated sisal fiber showed a tensile strength of 580 MPa, a Young´s modulus of 17 GPa and a density of 1.424 g/cm^3 [19,46]. On the other hand, according to the bibliography, the tensile strength, Young´s modulus and density of E-glass fiber are 3450 MPa, 72 GPa and 2.540 g/cm^3, respectively [47]. Hence, the specific strength and modulus ratios between glass fiber and treated sisal fiber are 3.3 and 2.4, respectively. Despite the specific strength ratio difference is considerable in fibers, the specific strength values in composites reinforced with sisal and glass fiber are similar. A possible reason for this could be that the adhesion of the PLA/PMMA matrix was stronger with NaOH treated sisal fibers than with glass fibers. Cousins et al. [22] studied the fractured surface of glass fiber reinforced PLA/PMMA composites by SEM and they observed pulled-out glass fibers of about 100 μm in length. Moreover, in contrast to our results, they observed that the glass fibers were not covered with the polymer matrix suggesting that fiber/matrix adhesion was really poor. Concerning the specific modulus values, the composite modulus is dependent on, among other parameters, the Young´s modulus of the reinforcement. The Young´s modulus of glass fibers is considerably higher than that of the treated sisal fibers. Therefore, the specific modulus of composites based on glass fibers is higher than composites based on NaOH treated sisal fibers. Regarding the elongation at break values, it was observed that the behavior of composites based on treated sisal fibers was slightly more ductile than those

composites based on chopped glass fibers manufactured by Cousins et al. [22]. It must be highlighted that the bio-based amount in composites prepared in the current study is at least 84 % in mass, whereas the bio-based amount in the composites prepared by Cousin et al. was lower than 60 % in mass.

On the other hand, DMA results can be used for estimating the heat deflection temperature (HDT) of materials, which is a critical parameter for the design of most industrial products [48,49]. The HDT is the upper limit temperature which the material can withstand without significant physical deformations under a specific load. Takemori established a correlation between the HDT and the temperature at which the Young´s modulus equals 0.75 GPa [50]. The Young´s modulus, E, can be calculated from the storage and loss modulus, E´ and E´´, respectively, according to Eq. (3):

$$E = 2(1+\upsilon)\sqrt{(E')^2 + (E'')^2} \quad (3)$$

where υ is the Poisson ratio and is assumed to be 0.33 which is typical for glassy polymers such as PLA and PMMA.

The estimated HDT of PLA/PMMA blend and its composites are shown in Table 2. After the addition of PMMA to neat PLA the HDT increased from 59.5 to 62.2 ºC. When 37 vol% treated sisal fiber was added to the PLA/PMMA blend the HDT increased up to 66.6 ºC. The main reason of this moderate HDT improvement is that fiber has higher HDT value than the matrix. In the literature the HDT improvement was observed for different reinforced thermoplastic composites [22,48,49,51,52]. Cousins et al. [22] estimated HDT from dynamic mechanical thermal analysis data for composites based on PLA/PMMA matrix and reinforced with chopped glass fibers. They observed that the HDT of PLA/PMMA blend (75/25 wt%) was around 79 ºC whereas the HDT of composites reinforced with 40 wt% (24 vol%) of chopped glass fibers was around 123.0 ºC. For comparison purposes, literature HDT values of different thermoplastic

composites are also reported in Table 2. The HDT values of PLA/PMMA composites prepared in the current study were similar to composites reinforced with calcium carbonate but lower than composites reinforced with glass fibers or talc. As the HDT values of composites prepared in the current work are low, an annealing process was carried out to increase the crystallinity of polymer matrix.

3.2. The effect of annealing process on the properties of PLA/PMMA-based systems

The annealing process was carried out at 105 ºC for 15 h in order to ensure that all samples were fully crystallized [53]. Figure 8 a-c illustrates the variation of the storage modulus, loss modulus and tan δ values of the PLA/PMMA blend and its composites after the annealing process. Similar to non-annealed counterparts, after the initial plateau region a storage modulus reduction was observed due to the chain mobility gained by the amorphous phase at the glass transition region. However, the reduction of modulus was not as significative as for non-annealed systems, inidicating a higher crystallinity degree. The absence of the cold-crystallization process indicated that the samples had completely crystallized during the previous annealing process. Therefore, the moduli values increased throughout all temperature range for all systems respect to non-annealed counterparts. After the annealing process, the tan δ peak height of neat PLA/PMMA blend and its composites reduced considerably due to the crystallization of PLA. On the contrary to the non-annealed counterparts, in annealed unreinforced PLA/PMMA samples two different T_g can be observed. The first one was located at 72 ºC and was related to a PLA-rich phase whereas the second one, located at 100 ºC, was related to a PMMA-rich phase. This fact corroborated that PLA and PMMA were partially miscible after the annealing process. On the other hand, in annealed composites the transition related to the PMMA-rich phase was not obvious and it was not possible

to determine the T_g of PMMA-rich phase whereas the T_g of the PLA-rich phase was located around 74-80 ºC.

Table 3 shows the estimated HDT values of PLA/PMMA blends and its composites after annealing using Eq. (3). HDT values of the PLA/PMMA polymer blend increased from 62.2 ºC to 86.8 ºC after the annealing process whereas the HDT of composites increased up to 102.3 ºC for 20 wt% of fiber loading. Shi et al. [49] and Bubeck et al. [54] observed that there was a significant increment of HDT of composites based on PLA polymer matrix after the annealing process. Shi et al. [49] studied the influence of heat treatment on the HDT of PLA/bamboo fiber composites. They observed that after the annealing process the composites based on 20 and 40 wt% fibers showed an increment of 11.8 ºC and 15.3 ºC, respectively. Furthermore, it can be observed in Table 3 that HDT of composites increased together with the fiber content, and composites based on 40 wt% showed the highest HDT value, 132.3 ºC. In composites, the main reason of the HDT improvement is that the crystallinity degree of the system was increased respect to non-annealed system counterparts. The obtained results suggested that fiber surface acted as nucleating sites since the higher the fiber content was, the higher was the HDT value. It was previously observed by polarized optical microscopy that the surface of sisal fibers acted as nucleating sites of PLA crystals creating a transcrystalline layer along the fiber surface, irrespective to the surface treatment applied [53].

After the annealing process the obtained HDT of composites were higher than composites based on PP and fillers (Table 2). However, the specific strength value of studied systems in the current study decreased, being the reduction more considerably for composites than for unreinforced matrix (Figure 9a). In composites, the strength, i.e., the maximum stress that a material can withstand, is strongly associated with the interfacial failure. Therefore, the strength value is sensitive to variations in interfacial

adhesion. The annealing process, damage the adhesion between the PLA/PMMA matrix and fibers and consequently the tensile strength value of composites was reduced. Although the specific strength reduced after the annealing process, the values are superior than the data reported in Table 2 for mineral filled polypropylene systems. The specific modulus value of polymer blend and its composites slightly increased after the annealing process (Figure 9b). The Young modulus, the ratio between stress and strain at linear region, is sensitive to variations in the crystallinity degree of the matrix. During the annealing process, the amorphous samples are capable to crystallize and consequently the modulus of composites increased. The crystallization of the polymer matrix resulted in an embrittlement of the samples and hence the elongation at break values decreased (Figure 9c). A similar trend was observed for PLA plasticized with 10 wt% vegetables oils and reinforced with 30 wt% NaOH treated sisal fibers [53].

Figures 10-11 show the SEM micrographs after the annealing process of the fractured surface of PLA/PMMA polymer blend and its composites at different magnifications. The annealing process created cracks (Figure 10b and Figure 11b) and seemed to damage the adhesion between the PLA/PMMA matrix and treated sisal fibers (Figure 11a) because more holes and pulled-out fibers were observed than in non-annealing composites (Figure 5a). Hence, these might be the reasons behind the reduction of the tensile strength value of composites after the annealing process.

4. Conclusions

Novel composites based on PLA/PMMA matrix and sisal fibers with at least of 84 wt% of bio-based materials were prepared and characterized. Compared to literature data of commercial mineral filled PP composites, in general, the specific tensile property values of composites based on PLA/PMMA matrix and treated sisal fibers were higher than those of mineral filled PP systems. After the annealing process, the estimated HDT

value of composites increased at least 38 ºC, depending on the amount of fiber content in the system. However, the specific strength values of composites decreased considerably because the fiber/polymer adhesion was damaged during the annealing process, and cracks were formed as observed by SEM micrographs. Although the PLA/PMMA blend reinforced with NaOH treated sisal fiber composites showed interesting specific tensile properties and HDT values after annealing process, the impact strength values of composites should be improved.

Acknowledgements

Authors are grateful for the financial support from the Basque Country Government in the frame of Elkartek "Provimat" KK-2018/00046 and PIBA19-0044 projects. The authors also thank for technical and human support provided by SGIker of UPV/ EHU and European funding (ERDF and ESF).

References

1. European Commission, 2013. Green Paper: On a European Strategy on Plastic Waste in the Environment. COM(2013) 123 Final, Brussels, Belgium.

2. Plastics Europe, EUPC, EPRO, EuPr, 2007. The Compelling Facts About Plastics. An analysis of plastics production, demand, and recovery for 2005 in Europe. https://www.plasticseurope.org/download_file/force/1576/181 (accessed, March 2019).

3. Bledzki AK and Jaszkiewicz A. Mechanical performance of biocomposites based on PLA and PHBV reinforced with natural fibres - A comparative study to PP .Compos Sci Technol 2010; 70: 1687-1696.

4. Kumar N and Das D. Fibrous biocomposites from nettle (Girardinia diversifolia) and poly(lactic acid) fibers for automotive dashboard panel application Compos Part B Eng 2017; 130: 54-63.

5. Oksman K, Skrifvars M and Selin JF. Natural fibres as reinforcement in polylactic acid (PLA) composites. Compos Sci Technol 2003; 63: 1317-1324.

6 Lu T, Liu S, Jiang M, Xiaoling X, Yong W, Zeyong W, Jan G, David H and Zuowan Z. Effects of modifications of bamboo cellulose fibers on the improved mechanical properties of cellulose reinforced poly(lactic acid) composites. Compos Part B Eng 2014; 62: 191-197.

7. Arbelaiz A, Fernandez B, Cantero G, Llano-Ponte R, Valea A and Mondragon I. Mechanical properties of flax fibre/polypropylene composites. Influence of fibre/matrix modification and glass fibre hybridization. Compos Part A-Appl Sci Manuf 2005; 36: 1637-1644.

8 Arbelaiz, A, Txueka, U, Mezo, I, Orue, A. Biocomposites Based on Poly(Lactic Acid) Matrix and Reinforced with Lignocellulosic Fibers: The Effect of Fiber Type and Matrix Modification. J. Nat Fibers 2020; DOI:10.1080/15440478.2020.1726247.

9 Fire-resistant flax-reinforced polypropylene/polylactic acid composites with optimized fire and mechanical performances Wiwat Pornwannachai, John Russell Ebdon, Baljinder K Kandola. J Thermoplast Compos Mater. doi.org/10.1177/0892705718815538

10 Sanadi AR, Caulfield DF, Jacobson RE, and Rowell RM. Renewable Agricultural Fibers as Reinforcing Fillers in Plastics: Mechanical Properties of Kenaf Fiber-Polypropylene Composites. Ind Eng Chem Res; 34: 1889-1896.

11. Wambua P, Ivens J and Verpoest I. Can they replace glass in fibre reinforced plastics? Compos Sci Technol 2003; 63: 1259-1264.

12 Manufacturing and characterization of sustainable hybrid composites using sisal and hemp fibres as reinforcement of poly(lactic acid) via injection moulding. Pappu, A, Pickering, K, Thakur, VK. Ind Crop Prod 2019; 137: 260-269.

13 Mechanical performance of thermoplastic olefin composites reinforced with coir and sisal natural fibers: Influence of surface pretreatment. Pereira, JF, Ferreira, DP, Bessa, J, Matos, J, Cunha, F, Araujo, I, Silva, LF, Pinho, E, Fangueiro, R. Polym Comp 2019; 40: 3472-3481.

14. Anakabe J, Zaldua Huici AM, Eceiza A and Arbelaiz A. Melt blending of polylactide and poly(methyl methacrylate): Thermal and mechanical properties and phase morphology characterization. J Appl Polym Sci 2015; 132: 42677 (1-8).

15. Arrieta MP, Fortunati E, Dominici F, López J and Kenny JM. Bionanocomposite films based on plasticized PLA-PHB/cellulose nanocrystal blends. Carbohydr Polym 2015; 121: 265-275.

16. Bouzouita A, Samuel C, Notta-Cuvier D, Odent J, Lauro F, Dubois P and Raquez JM Design of highly tough poly(l -lactide)-based ternary blends for automotive applications. J Appl Polym Sci 2016; 133: 43402 (1-9).

17. Navarro-Baena I, Sessini V, Dominici F, Torre L and Kenny JM and Peponi L. Design of biodegradable blends based on PLA and PCL: From morphological, thermal and mechanical studies to shape memory behavior. Polym Degrad Stab 2016; 132: 97-108.

18. Orue A, Eceiza A and Arbelaiz A. Preparation and characterization of poly(lactic acid) plasticized with vegetable oils and reinforced with sisal fibers. Ind Crop Prod 2018; 112: 170-180.

19. Orue A, Jauregi A, Unsuain U, Labidi J, Eceiza A and Arbelaiz A. The effect of alkaline and silane treatments on mechanical properties and breakage of sisal fibers and poly(lactic acid)/sisal fiber composites. Compos Part A Appl Sci Manuf 2016; 84: 186-195.

20. Quiles-Carrillo L, Montanes N, Sammon C, Balart R, Torres-Giner S. Compatibilization of highly sustainable polylactide/almond shell flour composites by reactive extrusion with maleinized linseed oil. Ind Crop Prod 2018; 111: 878-888.

21. Anakabe J, Zaldua Huici AM, Eceiza A and Arbelaiz A. The effect of the addition of poly(styrene-co-glycidyl methacrylate) copolymer on the properties of polylactide/poly(methyl methacrylate) blend. J Appl Polym Sci 2016; 133: 43935 (1-10).

22. Cousins DS, Lowe C, Swan D, Barsotti R, Zhang M, Gleich K, Berry D, Snowberg D, Dorgan JR. Miscible blends of biobased poly(lactide) with poly(methyl methacrylate): Effects of chopped glass fiber incorporation. J Appl Polym Sci 2017;134: 44868 (1-12).

23. Mondragon G, Fernandes S, Retegi A, Peña C, Algar I, Eceiza A and Arbelaiz A. A common strategy to extracting cellulose nanoentities from different plants. Ind Crop Prod 2014; 55: 140-148.

24 Wise, LE, Murphy, M, D'Addieco, AA. Chlorite holocellulose, its fractionation and bearing on summative wood analysis and on studies on the hemicelluloses. Pap Trade J 1946; 112: 35-43.

25 Rowell RM, Pettersen R, Han JS, Rowell JS, Tshabalala MA. Chapter 3, pg 35-74, of Handbook of Wood Chemistry and Wood Composites 2005.

26. Orue A, Jauregi A, Peña-Rodriguez C, Labidi J, Eceiza A, Arbelaiz A. The effect of surface modifications on sisal fiber properties and sisal/poly (lactic acid) interface adhesion. Compos Part B Eng 2015; 73; 132-138.

27. Truong M, Zhong W, Boyko S and Alcock M. A comparative study on natural fibre density measurements. J Text Inst 2009; 100: 525-529.

28. Fischer BEW, Sterzel HJ and Wegner G. Investigation of the structure of solution grown crystals of lactide copolymers by means of chemicals reactions. Kolloid-Z. Z. Polym. 1973; 251: 980-990.

29 Tensile and water absorption properties of solvent cast biofilms of sugarcane leaves fibre-filled poly(lactic) acid. Nanthakumar, K, Yeng, CM, Chun, KS. J Thermoplast Compos Mater 2020; 33; 289-304.

30 Arbelaiz A, Fernández B, Ramos JA, Retegi A, Llano-Ponte R and Mondragon I. Mechanical properties of short flax fibre bundle/polypropylene composites: influence of matrix/fibre modification, fibre content, water uptake and recycling. Compos Sci Technol 2005; 65: 1582-1592.

31. Nam TH, Ogihara S, Tung NH and Kobayashi S. Effect of alkali treatments on interfacial and mechanical properties of coir fiber reinforced poly(butylene succinate) biodegradable composites. Compos Part B Eng 2011; 42: 1648-1656.

32. Huda MS, Drzal LT, Mohanty AK and Misra M. Chopped glass and recycled newspaper as reinforcement fibers in injection molded poly(lactic acid) (PLA) composites: A comparative study. Compos Sci Technol 2006; 66: 1813-1824.

33. Yuryev Y, Mohanty AK and Misra M. Novel biocomposites from biobased PC/PLA blend matrix system for durable applications. Compos Part B Eng 2017; 130: 158-166.

34 Park B and Balatinecz JJ. Mechanical properties of wood-fiber/toughened isotactic polypropylene composites. Polym Compos 1997; 18: 79-89.

35. Bledzki AK, Jaszkiewicz A and Scherzer D. Mechanical properties of PLA composites with man-made cellulose and abaca fibres. Compos Part A Appl Sci Manuf 2009; 40: 404-412.

36. Pérez-Fonseca AA, Robledo-Ortíz JR, González-Núñez R and Rodrigue D. Effect of thermal annealing on the mechanical and thermal properties of polylactic acid-cellulosic fiber biocomposites. J Appl Polym Sci 2016; 133: 43750 (1-9).

37. Imre B, Renner K and Pukánszky B. Interactions, structure and properties in poly (lactic acid)/thermoplastic polymer blends. Express Polym Lett 2014; 8: 2-14.

38. Hao X, Kaschta J, Pan Y, Liu X and Schubert DW. Intermolecular cooperativity and entanglement network in a miscible PLA/PMMA blend in the presence of nanosilica. Polymer 2016; 82: 57-65.

39. Li SH and Woo EM. Immiscibility-miscibility phase transitions in blends of poly/L-lactide) with poly(methyl methacrylate). Polym Int 2008; 57: 1242-1251.

40 Khoo, RZ, Chow, WS. Mechanical and thermal properties of poly(lactic acid)/sugarcane bagasse fiber green composites. J Thermoplast Compos Mater 2017; 30: 1091-1102.

41. Mathew AP, Oksman K and Sain M. The effect of morphology and chemical

characteristics of cellulose reinforcements on the crystallinity of polylactic acid. J Appl Polym Sci 2006; 101: 300-310.

42. Samuel C, Cayuela J, Barakat I, Müller AJ, Raquez JM and Dubois P. Stereocomplexation of polylactide enhanced by poly(methyl methacrylate): Improved processability and thermomechanical properties of stereocomplexable polylactide-based materials. ACS Appl Mater Interfaces 2013; 5: 11797-11807.

43 Coskun K, Mutlu A, Dogan M, Bozacı E. Effect of various enzymatic treatments on the mechanical properties of coir fiber/poly(lactic acid) biocomposites. J Thermoplast Compos Mater doi.org/10.1177/0892705719864618

44 Product datasheets for standard polypropylene (PP) compounds – RTP Company. http://web.rtpcompany.com/info/data/0100/index.htm (accessed March, 2019)

45. Toro P, Quijada R, Peralta R and Yazdani-Pedram M. Influence of grafter polypropylene on the mechanical properties of mineral-filled polypropylene composites. J Appl Polym Sci 2007; 103: 2343-2350.

46. Orue A, Eceiza A, Peña-Rodriguez C and Arbelaiz A. Water uptake behavior and Young modulus prediction of composites based on treated sisal fibers and Poly(lactic acid). Materials 2016; 9: 400 (1-14).

47. Chen Q, Linghu T, Gao Y, Wang Z, Liu Y, Du R and Zhao G. Mechanical properties in glass fiber PVC-foam sandwich structures from different chopped fiber interfacial reinforcement through vacuum-assisted resin transfer molding (VARTM) processing. Compos Sci Technol 2017; 144: 202-207.

48. Luo H, Zhang C, Xiong G and Wan Y. Effects of alkali and alkali/silane treatments of corn fibers on mechanical and thermal properties of its composites with polylactic acid. Polym Compos 2016; 37: 3499-3507.

49. Shi QF, Mou HY, Li QY, Wang JK and Guo WH. Influence of heat treatments on the heat distortion temperature of poly(lactic acid)/bamboo fiber/talc hybrid biocomposites. J Appl Polym Sci 2011; 123: 2828-2836.

50. Takemori MT. Towards an understanding of the heat distortion temperature of thermoplastics. Polym Eng Sci 1979; 19: 1104-1109.

51. Kim KW, Lee BH, Kim HJ, Srirtoth K and Dorgan JR. Thermal and mechanical properties of cassava and pineapple flours-filled PLA bio-composites. J Therm Anal Calorim 2018, 108, 1131-1139.

52. Xie S, Zhang S, Wang F, Liu H and Yang M. Influence of annealing treatment on the heat distortion temperature of nylon-6/montmorillonite nanocomposites. Polym Eng Sci 2005; 45: 1247-1253.

53. Orue A, Eceiza A and Arbelaiz A. The effect of fiber surface treatments, plasticizer addition and annealing process on the crystallization and the thermo-mechanical properties of poly(lactic acid) composites. Ind Crop Prod 2018; 118: 321-333.

54. Bubeck RA, Merrington A, Dumitrascu A and Smith PB. Thermal analyses of poly(lactic acid) PLA and micro-ground paper blends. J Therm Anal Calorim 2018; 131: 309-316.

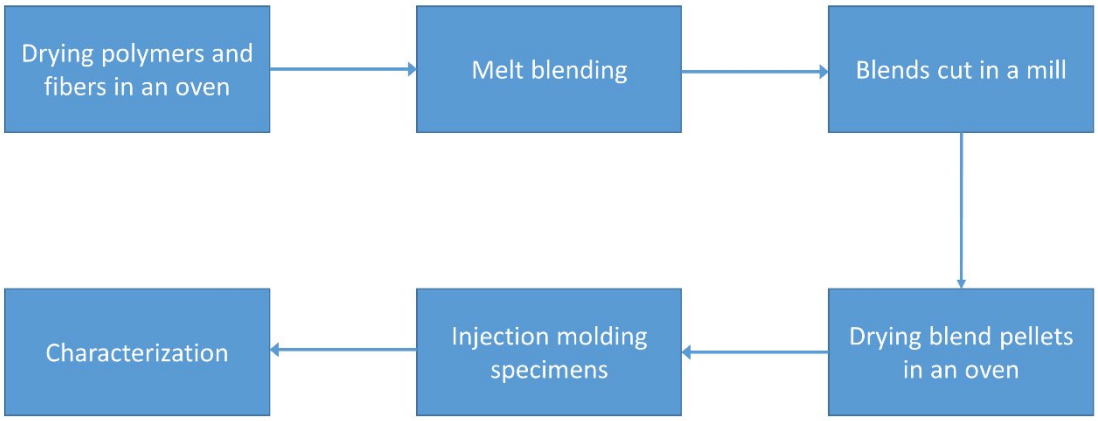

Figure 1. The schemetic diagram of different steps involved in the manufacturing of composites.

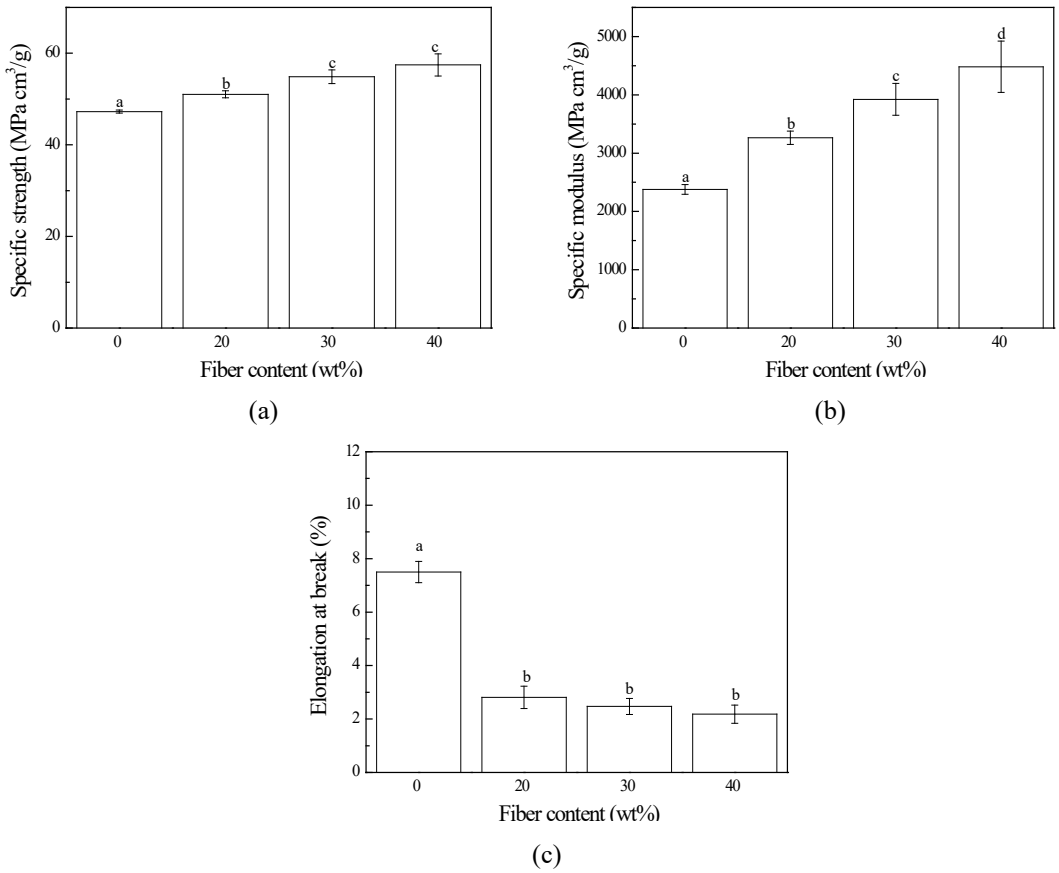

Figure 2. Specific tensile properties of unreinforced PLA/PMMA blend and its composites: (a) specific strength, (b) specific modulus and (c) elongation at break values. * Values with different letters are significantly different ($P < 0.05$) through the Tukey's multiple range test.

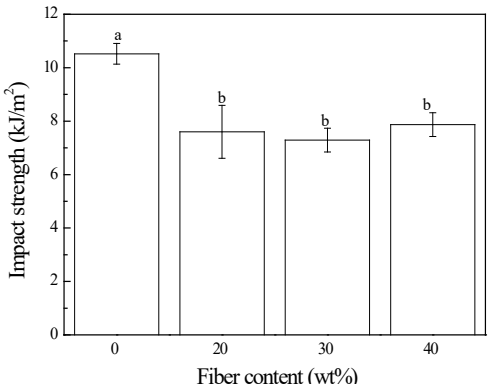

Figure 3. Impact strength values of unreinforced PLA/PMMA blend and its composites.

* Values with different letters are significantly different ($P < 0.05$) through the Tukey's multiple range test.

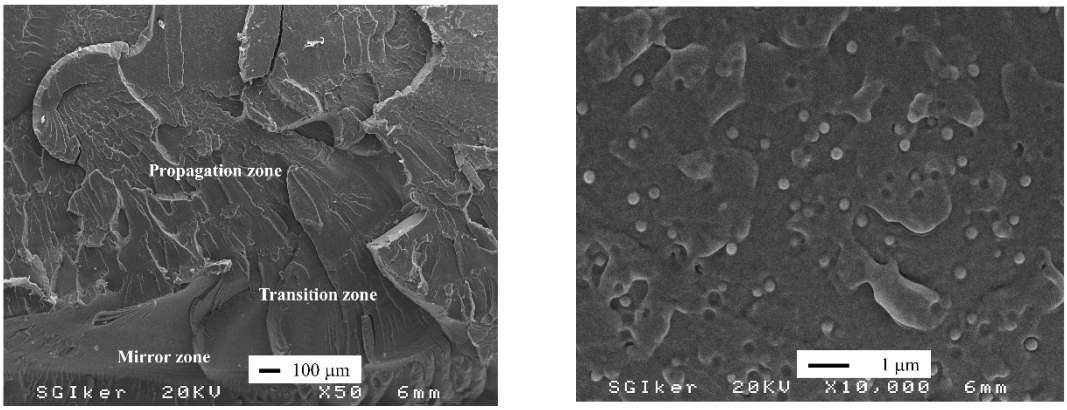

(a) (b)

Figure 4. SEM micrographs of impact fractured surface of unreinforced PLA/PMMA blend at different magnifications: (a) x50 and (b) x10000.

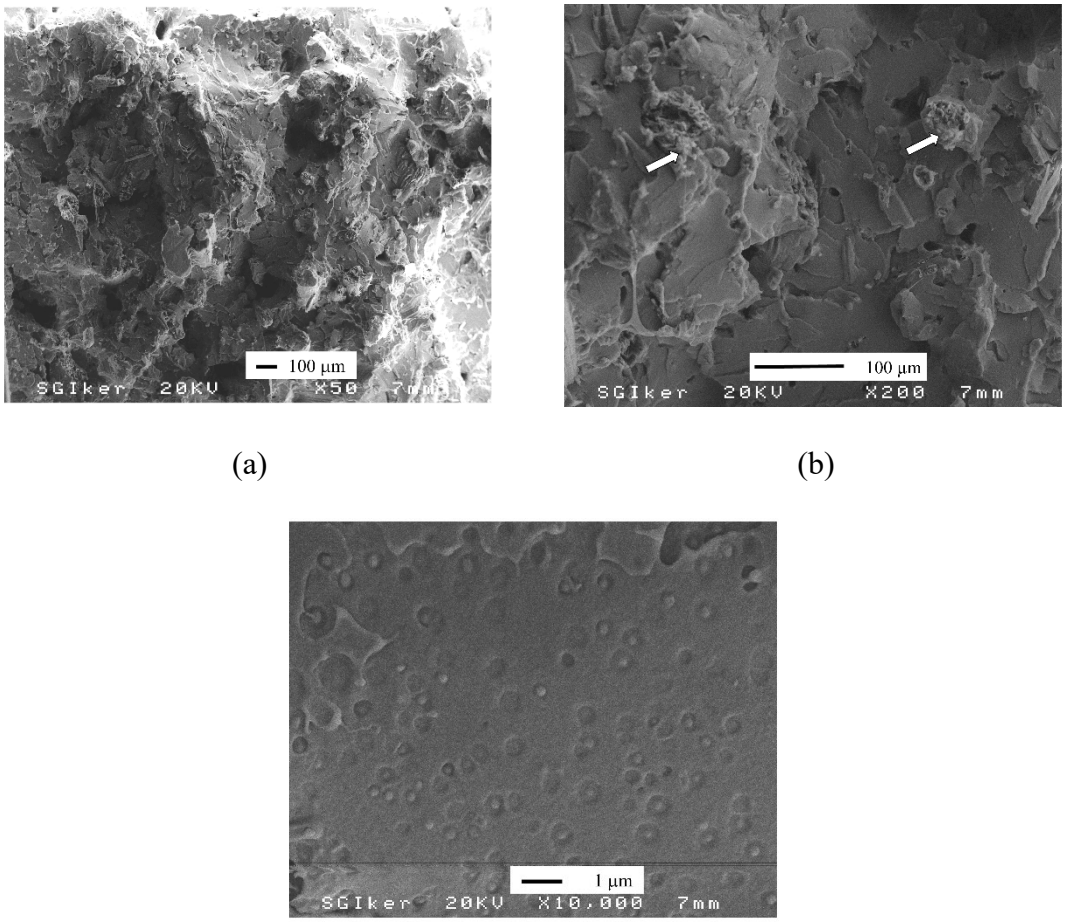

(a) (b)

(c)

Figure 5. SEM micrographs of impact fractured surface of composite with 30 wt% treated sisal fibers at different magnifications: (a) x50, (b) x200 and (c) x10000.

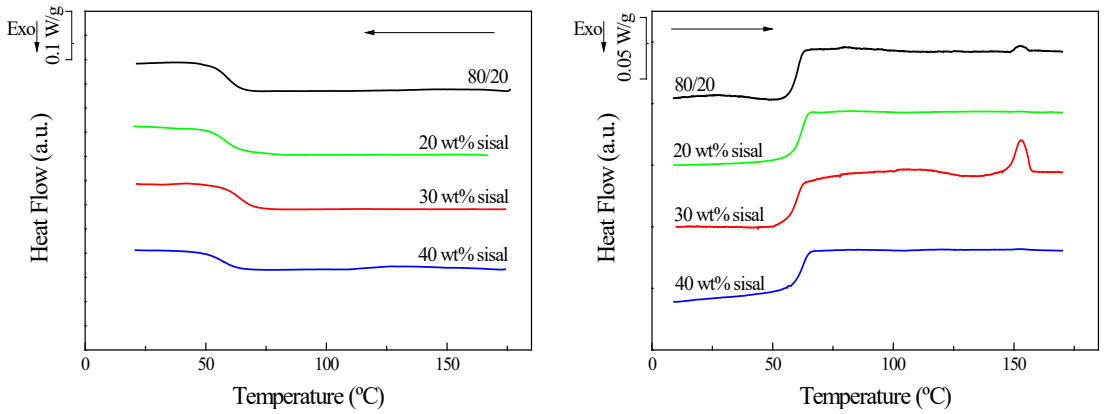

(a) (b)

Figure 6. (a) Cooling and (b) second heating scan of DSC thermogram of unreinforced PLA/PMMA blend and its composites.

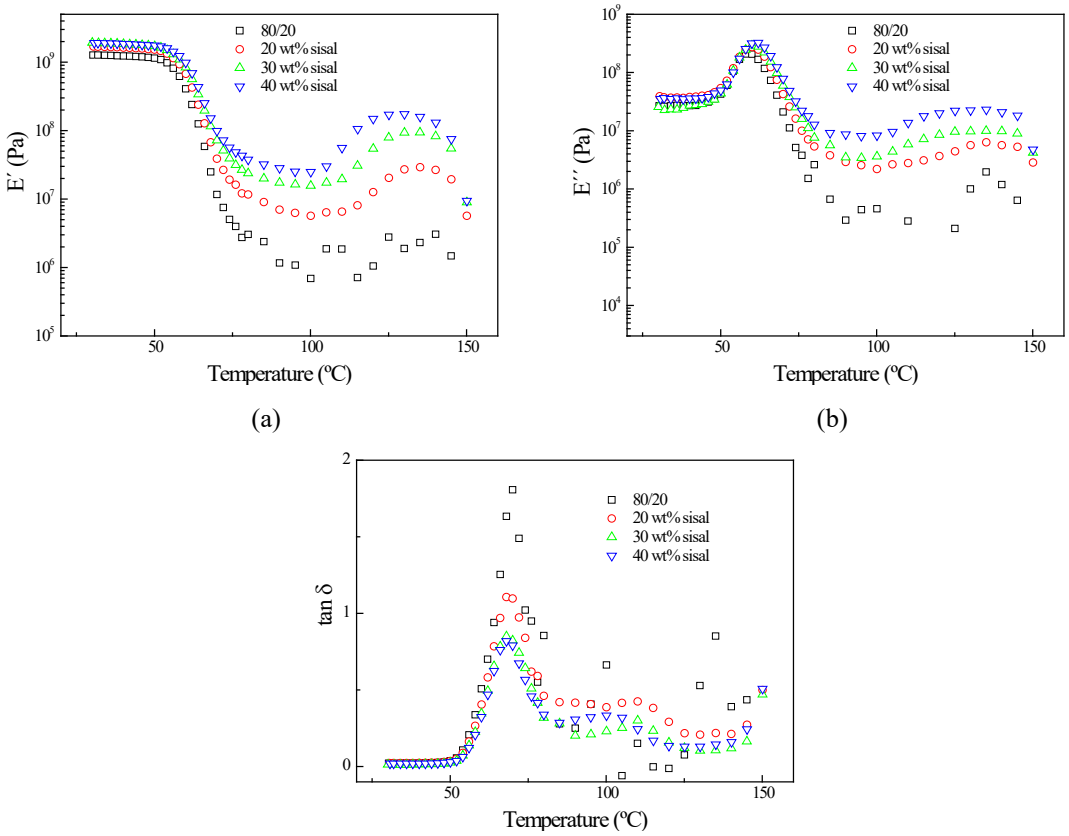

Figure 7. (a) Storage modulus, (b) loss modulus and (c) tan δ values of unreinforced PLA/PMMA blend and its composites.

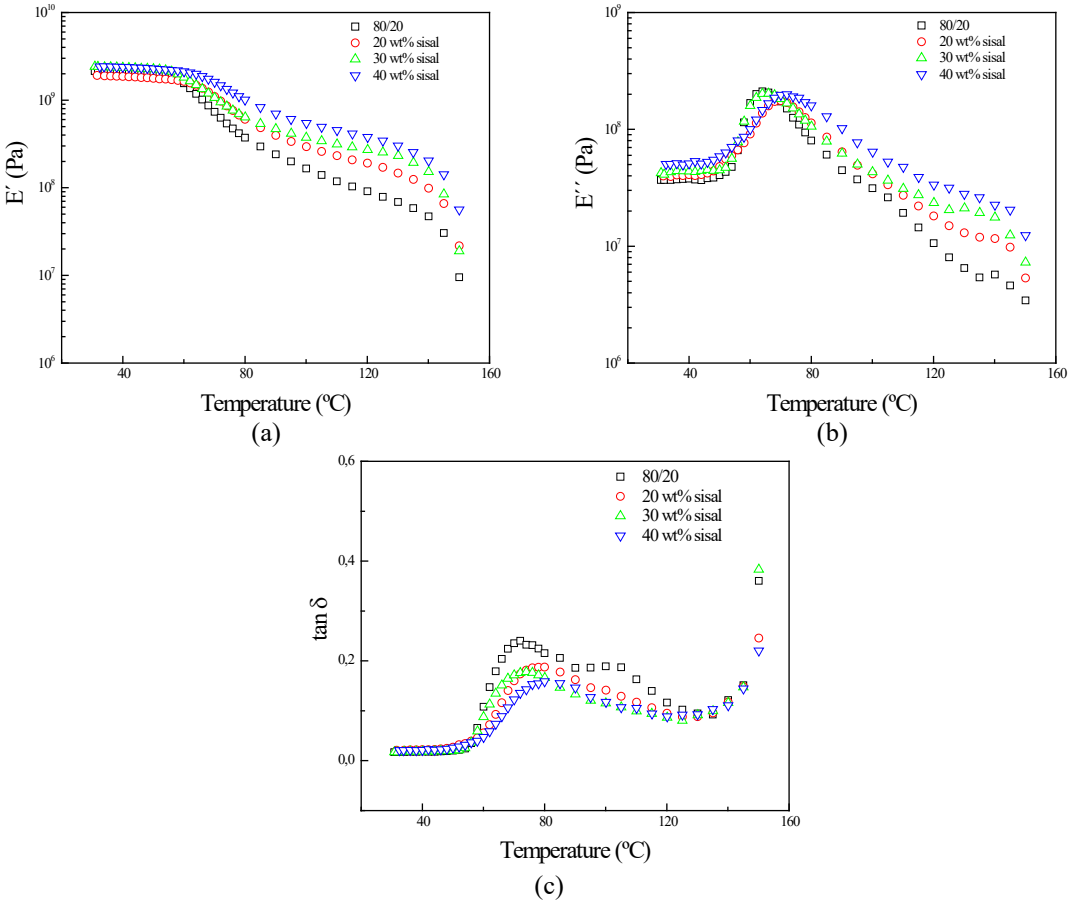

Figure 8. (a) Storage modulus, (b) loss modulus and (c) tan δ values of unreinforced PLA/PMMA blend and its composites after annealing process.

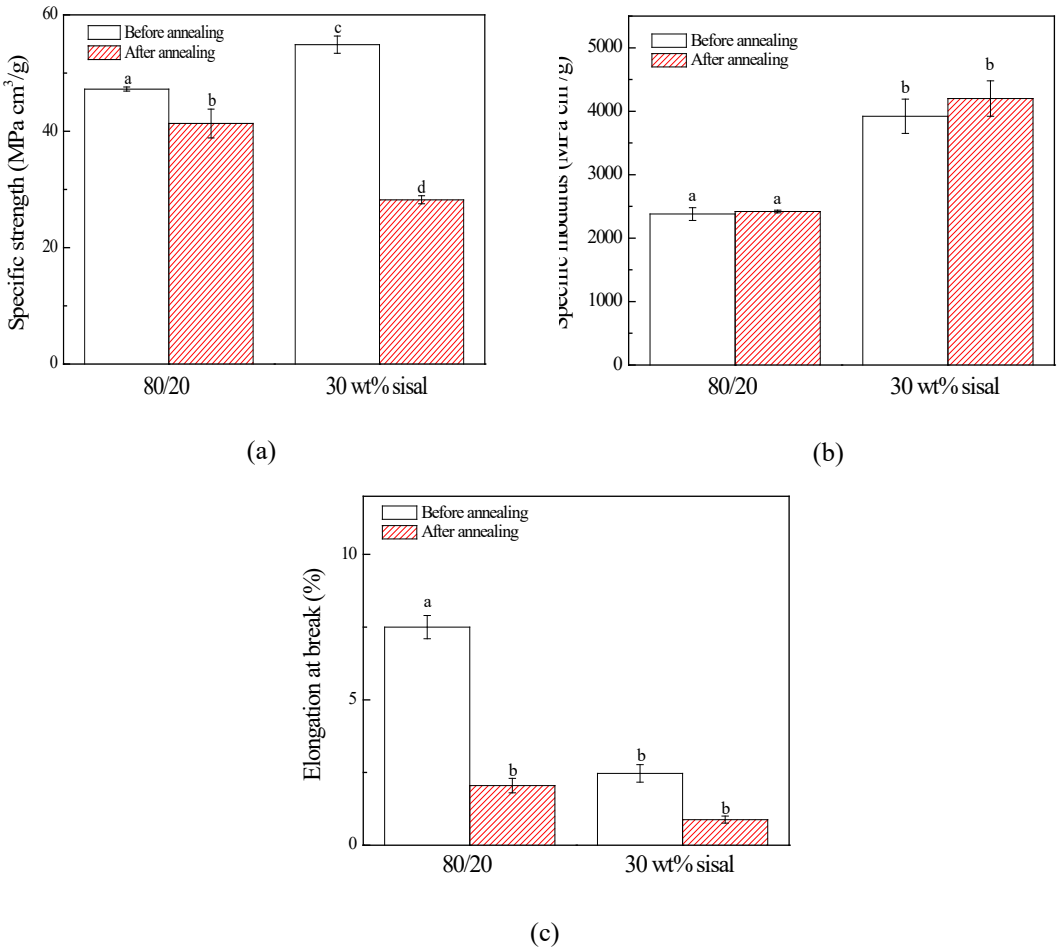

Figure 9. Specific tensile properties of unreinforced PLA/PMMA blend and its composites before and after annealing process: (a) specific strength, (b) specific modulus and (c) elongation at break values. * Values with different letters are significantly different ($P < 0.05$) through the Tukey's multiple range test.

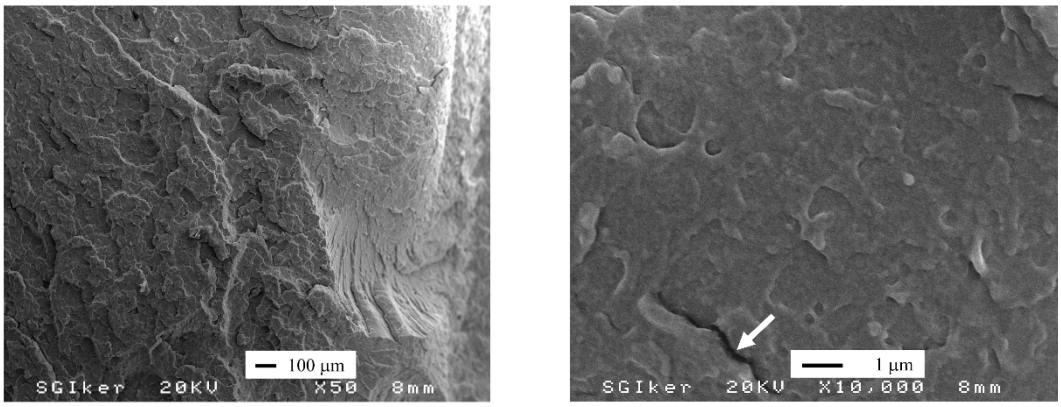

(a) (b)

Figure 10. SEM micrographs of fractured surface of unreinforced PLA/PMMA blend at different magnifications: (a) x50 and (b) x10000.

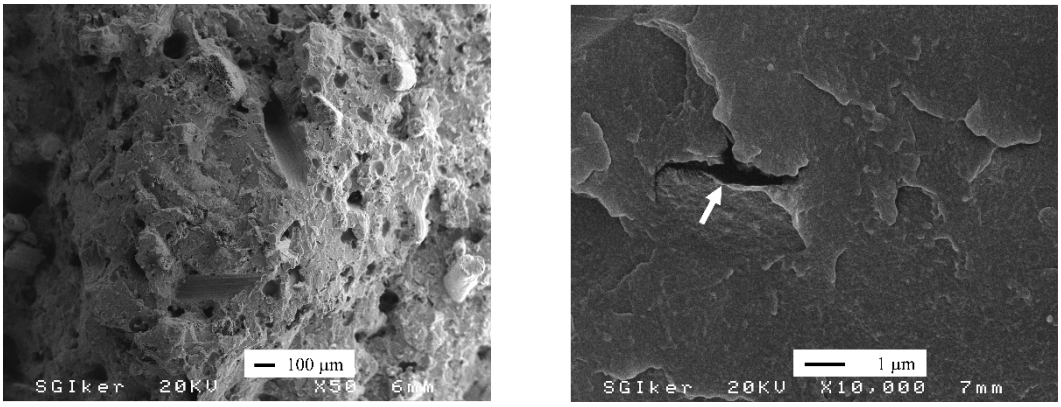

(a) (b)

Figure 11. SEM micrographs of fractured surface of composites based on 30 wt% treated sisal fibers at different magnifications: (a) x50 and (b) x10000.

System	Length (μm)	Diameter (μm)
20 wt% sisal	394.8 ± 5.5[a]	23.0 ± 0.8[a]
30 wt% sisal	266.2 ± 7.1[b]	22.2 ± 0.7[b]
40 wt% sisal	190.4 ± 0.8[c]	20.9 ± 0.2[c]

Table 1. Mean length and mean diameter values after processing (obtained from Log Normal and Gaussian frequency distribution, respectively) and the aspect ratio l/d of sisal fibers. * Values within each column with different letter are significantly different ($P < 0.05$) through the Tukey's multiple range test.

System	Reinforcement volume fraction (%)	Specific strength (MPa cm^3/g)	Specific modulus (MPa cm^3/g)	Deformation at break (%)	HDT (ºC)	Reference
PLA	0	52.8 ± 1.3	3097 ± 388	2.4 ± 0.3	59.5 (*)	14
PLA/PMMA (80/20)	0	47.3 ± 0.4	2378 ± 102	8.2 ± 1.3	62.2 (*)	Current study
PLA/PMMA (75/25)	0	48.8 ± 2.0	3374 ± 275	1.5 ± 0.4	79.0 (*)	18
PLA-treated sisal fiber	16	51.0 ± 2.5	4994 ± 318	1.8 ± 0.2	60.1 (*)	14
PLA-glass fiber	17	49.6 ± 1.0	4141 ± 247	1.8	73.9	25
PP-mica	17	22.8	5045	9.0	---	35
PLA/PMMA-treated sisal fiber	18	51.0 ± 1.0	3262 ± 145	2.8 ± 0.4	64.4 (*)	Current study
PP-talc	18	25.1 ± 1.0	1839 ± 160	3.0	---	36
PP-talc	18	24	4137	>10	82.0	35
PP-$CaCO_3$	18	20.2 ± 1.0	1456 ± 40	17	---	36
PP-$CaCO_3$	18	18.7	2523	>10	68.0	35
PLA-treated sisal fiber	24	57.0 ± 2.7	5467 ± 570	1.5 ± 0.1	61.3 (*)	14
PLA/PMMA-glass fiber	24	54.6 ± 5.1	7941 ± 550	1.4 ± 0.4	123.0 (*)	18
PLA/PMMA-treated sisal fiber	27	54.9 ± 1.9	3924 ± 355	2.5 ± 0.3	65.6 (*)	Current study
PLA-bamboo fiber	35	---	---	---	53.2	40
PLA-flax fiber	36	31.7 ± 5.5	5383 ± 369	0.9 ± 0.2	---	5
PLA/PMMA-treated sisal fiber	37	57.4 ± 3.2	4482 ± 578	2.2 ± 0.3	66.6 (*)	Current study

(*) Values estimated from DMA data

Table 2. The properties of PLA/PMMA based systems and other thermoplastic composites.

	Estimated HDT (ºC)		Increment
System	**Before annealing**	**After annealing**	**(ºC)**
80/20	62.2	86.8	24.6
20 wt% sisal	64.4	102.3	37.9
30 wt% sisal	65.6	117.9	52.3
40 wt% sisal	66.6	132.3	65.6

Table 3. The HDT of PLA/PMMA blend and its composites before and after annealing process.